

Impact of jet impingement on a flat bed of particles and scour hole development mechanism in Newtonian and non-Newtonian fluids

A. H. Rabenjafimanantsoa and Rune W. Time

University of Stavanger, Norway

ABSTRACT

The impact of an axisymmetric liquid jet on granular beds has been studied experimentally in both Newtonian and non-Newtonian fluids. The liquid jet is ejected from a nozzle and impinges normally to a flat bed of non-cohesive polydisperse glass beads. A scour hole or a crater is formed in the bed caused by the jet impingement. The scour pattern, shape diameter and depth are studied as functions of jet velocity and nozzle distance above the bed.

High-speed video imaging was used to obtain a detailed analysis of the flow and the development of the scour hole patterns ("washout craters"). Particle Image Velocimetry (PIV) technique is calculating velocity profiles and turbulence characteristics of the jet flows. The bed erosion start from an initially plane bed, but develops quickly from the stagnation point of the jet into the steady circularly shaped washout crater. The turbulent flow profiles then also finds a steady overall shape in the interaction with the crater and the surrounding bed. Due to the spread in size distribution of the glass particle beads, even when a steady bed is present, smaller particles can stay entrained in the flow. The entrainment eventually stops when the flow velocity is lower than the excitation and lift velocity of the particles. For sufficiently high jet velocity there is a

steady exchange of particles between the bed and the fluid flow field, which over long times can lead to particle size sorting of the bed which surrounds the crater. Both the scour pattern and the entrained particle fraction are strongly dependent on the liquid rheology.

INTRODUCTION

Jet impingement on a surface is an effective and flexible way for mass or energy transfer in many industrial applications. This can be achieved efficiently by the transfer of large amounts of thermal or mass between the surface and the fluid¹. A large amount of information on the general use and performance of impinging jets is reviewed thoroughly by Zuckerman and Lior¹.

Recently, investigators have studied experimentally the vertical impingement of a jet upon sediments². They examined the deepening and spreading of the crater in the sediments by using light attenuation and depositometer. They observed the crater to deepen at a near-constant speed while the crater radius remained constant.

In oil and gas well drilling limited attention exists on jet impingement on the reservoir formation although the drill bit represents the heart of the drill string. As the drill bit rotates during drilling cuttings

are produced and needs to be removed. Drilling fluid is pumped to the drill pipe and to the bit³. It then passes out through the jetting nozzles of the bit at high velocity and picks up the drill cuttings and cleans the bit. To the authors knowledge the literature addressed to the impact of the jet dynamics in oil and gas reservoir formation is very poor. It then necessitates studies which has been neglected by bit companies. Rather, more information on nozzle placement, design are available. In oil well drilling numerous tests have been made to improve the hydraulics efficiency beneath the drill bit.

DYNAMICS OF JET IMPINGEMENT

Beltaos and Rajaratnam⁴ illustrated the distinct impingement regions of flow based on an axisymmetric, circular jet, as seen in Fig. 1.

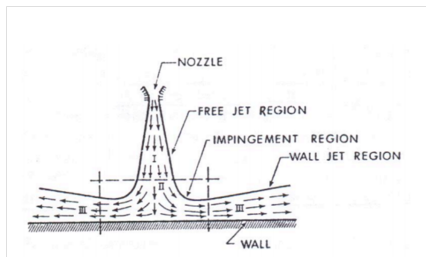


Figure 1: Regions of the jet impingement on a flat particle bed.

It is axisymmetric, circular with three distinct regions of flow. The first region is the free jet region. No effect on the impingement is considered here. The second is the impingement region. Here, deceleration of the jet is significant. The jet trajectory is directed from the axial direction to the radial direction. The third is the wall jet region where the radial distance from the impingement grows. When beds of particles are exposed to shear by a carrier fluid they are deformed, and dunes or ripples are commonly generated at low velocities. Dunes exert a significant influence on the flow process, such as frictional pres-

sure drop, erosion and deposition⁵. Regarding particle motion one may distinguish between saltation and creep. During creep, particles are moving by rolling or climbing/sliding, as illustrated in Fig. 2 along the bed, while during saltation, particles are moving by hopping along the bed repeatedly.

An other situation of liquid jet flow in bed of particles processes involves bed changes on the impingement region as the jet velocity is increased. This bed deforms and ultimately a crater is formed. The particle erosion is driven by turbulent shear stress and can be quantified by the turbulent kinetic energy of the flow, according to Haehnel et al.⁶.

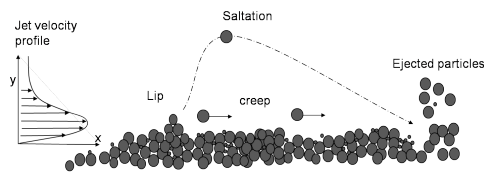


Figure 2: Cartoon of saltating and creep particles.

Figure 3 illustrates a vortex which is a primary driver of particle motion and uplift. The vortex passes above the particles and increases shear as it uplifts the particles from the bed. The violent velocity of the vortex is trapping the particles and the heavier particles are spun out due the action of centrifugal forces. The smaller

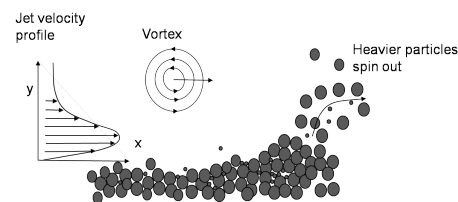


Figure 3: Cartoon of vortex trapping.

particles are extracted from the flow and transported as well as near the bed and into suspension. Generally, most of the

smaller particles stay in suspension in a period of time during the flow.

EXPERIMENTAL

Experimental setup

Figure 4 shows a schematic representation of the setup. The experiments were

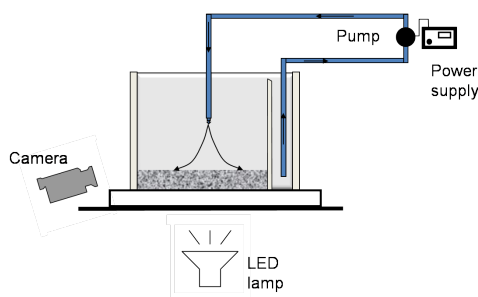


Figure 4: Experimental setup.

conducted using a glass cell of 190mm x 190mm x 200mm (BxLxH). This setup was put on top of a transparent glass to have visibility access from the bottom of the glass cell. The glass cell is separated in two chamber by an acrylic plate. A gear pump was used for recirculating the system. A filter was placed at the inlet of the pump to avoid particles from being sucked in to the pump. This served as a separation of the particles from being sucked in to the pump. The experimental fluids used are water and water based polymer solutions. The system can be divided in two regions. In the bottom region of the cell non-cohesive polydisperse glass beads is placed to act as particles bed. The bed height is 3.2cm. Glass bead particles of 200-300 μm were used with density of 2.594 g/ml. The experiments have been performed with the glass beads as shown in Fig. 5. In the upper region water or water based polymer solutions was used as fluids. The polymer solution is Poly Anionic Cellulose (PAC) dissolved in water.

At the top of the box, a 0.31cm diameter nozzle was mounted 8.3cm above the

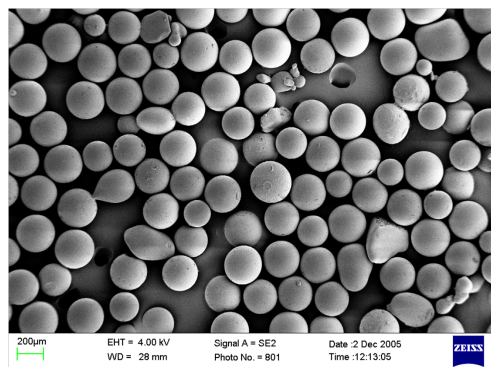


Figure 5: Picture of glass bead particles used in the experiment. The density of the particle is 2.594 g/ml.

bed. In all experiments this height was sufficient to create an erosion pattern which could be measured using a millimeter paper placed beneath the box. The flow was controlled using voltage readings, a Manson SPS9602 power supply. Before the experiments the pump was calibrated with a Mettler Toledo ID1 weight equipment.

The images were obtained using a low cost camera (Samsung EK-GC 100, 768 x 512 pixels 120fps in slow motion video mode) and LED lamps. This is a simple and inexpensive system that probably can substitute expensive equipment to achieve high accuracy as compared with high cost and complex system. The LED lamps are directed from the bottom to achieve visibility of the crater.

Fluid rheology

The fluid used is water and Poly Anionic Cellulose (PAC) dissolved in water. 2 and 4 g/L of PAC were mixed for a day and then allowed to set for a day before use. The rheological characterization of the polymeric solutions was done using an Anton Paar MCR-302 for shear rates ranging from 1 to 1020 s^{-1} . Cone plate geometry CP50-1 was used for performing the experiments at 20°C. The measurements were repeated several times to get rid of

experimental uncertainty. The viscosity as a function of shear rate is graphed in Fig. 6 for these two solutions. It can be seen from this figure that the polymer solutions are shear thinning.

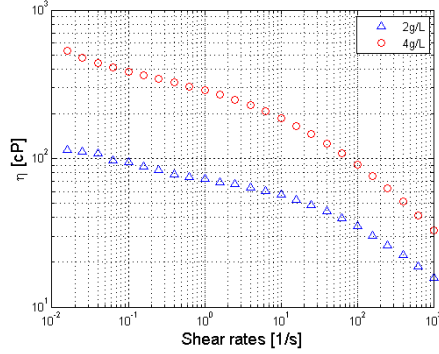


Figure 6: Loglog plot of viscosity versus shear rate at 20°C of the 2g/L and 4g/L concentrations of PAC dissolved in water.

PIV analysis

After being recorded in slow motion mode from the Samsung camera, i.e. 120 fps, the images were extracted using the Avidemux software⁷ and saved for further processing. An open source PIVlab version 1.4 has been used for post processing the images. It is a time-resolved particle image velocimetry (PIV) software that does not only calculate the velocity distribution within particle image pairs, but can also be used to derive, display and export multiple parameters of the flow pattern. A user-friendly graphical user interface (GUI) makes PIV analysis and data post-processing fast and efficient⁸. Up to 300 images were extracted for the PIVlab analysis. This was chosen to allow affordable calculation time. PIVlab performs cross correlation between pair of images. The size of the interrogation area was set to 64x64 pixels with 50% overlap.

EXPERIMENTAL RESULTS

The focus of this study was also to compare between Newtonian and non-

Newtonian fluid on the impingement of the jet onto particles bed. Therefore, water was first used and presented as reference fluid. The 4g/L of PAC dissolved in water was tested first and made particles in suspension for a long time. It was then decided to use the 2g/L of PAC dissolved in water which was considered to give an overall picture for this comparison.

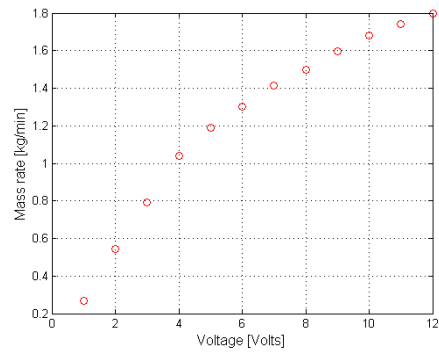


Figure 7: Mass flow rate vs. Voltage reading

The experiments started from an initially flat bed. The jet was then run for a short period of time and the erosion pattern gradually takes place. Voltage readings were used for controlling the jet velocities. Experiments were taken for 1, 2.1, 2.6, 3, 4.1 and 5 Volts. Fig. 7 shows the relationship between mass rate exerted by the gear pump as a function of voltage readings. It can be seen from Fig. 7 that from 1 to approximately 5volts a linear relationship between mass rate and voltage reading is observed. Therefore, the experiments were limited within this range of voltage reading to allow repeatability.

As seen from Fig. 8 when the jet is impacted the bed surface the following events could describe the different events during this event:

- the fluid from the impingement region is downwashing to the bed at $t = 0s-371ms$. Some sliding/creeping particles are following along the bed, as illustrated in Fig. 2. This situation is

similar with dune transport in pipes⁵.

- eroded particles are saltating, uplifted and ejected outward at $t = 640$ ms. Particles are hopping around the bed and trapped in vortex as illustrated in Fig. 3. New downwashing event is starting
- while the bed is eroded and particles ejected a new ejection of particles is starting at $t = 876$ ms particles. This makes the scour pattern take the form of a crater as seen in Fig. 9
- due to the confinement of the glass cell walls the particles are trapped and turn upward. This situation drives the flow circulation from the wall back to the impingement region

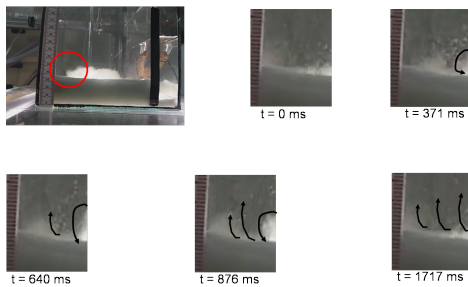


Figure 8: Extracted image sequences of the outwash and ejection of particles. The detail of time sequences of the encircled area is shown. The arrows represent the direction of the flow. The fluid is water.

- a new crater is formed and these events will continue over and over again.

The scour is radially varying and symmetric about the jet axis. Fig. 9 shows an example of erosion due to the jet impingement on the immersed bed. LED light was set below the setup. This is the typical scour pattern in these experiments. It can be seen that there exists two distinctive craters during the jet impingement. One is close to the jet axis approximately 20mm in diameter where there is free for particle

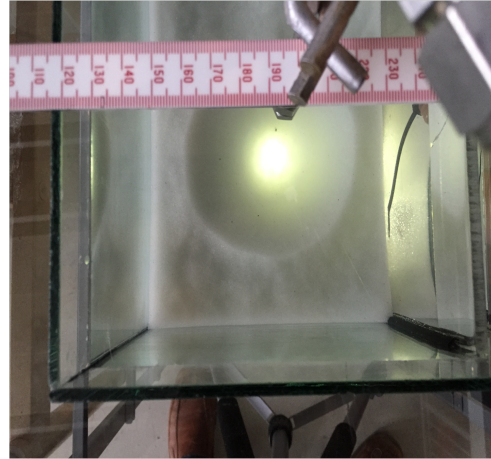


Figure 9: Top view of the scour pattern in the particle bed after the jet has been running. LED light is set from below.

bed. The other is approximately 60mm in diameter.

Overall, the particles were ejected away leaving zones of crater. When the jet velocity was low the particles started to roll and bounce on top of each other. Close to the jet axis, there was little to no observable particles activities. However, saltation was observed above the particle bed that gradually thickened along the surface. At higher jet velocity the particles were concentrated in the outer region as the crater became bigger. Heavier particles were uplifted and spun out while smaller particles were trapped into a vortex and kept into suspension.

For jet mean velocity of 0.3m/s experiments 20 images have been extracted and imported to PIVLab. Due to insufficient image frames and seeding particles some noises and erroneous vectors were observed and averaged out. Nevertheless, PIVLab could provide a profile plot of the vertical component of the jet velocity profile for the scour development on the line, as shown in Fig. 10.

It can be seen from Fig. 10 that the vertical component of the jet velocity is at its maximum approximately in the middle

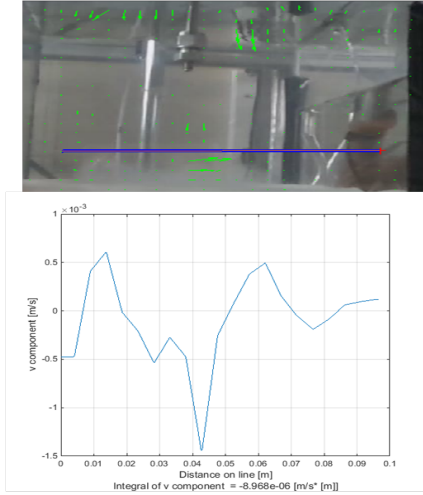


Figure 10: Top: Reference picture showing a line situated at 1.5 cm above the bed. Bottom: Profile plot of the vertical component of the jet velocity. Voltage reading 4.1 volts.

of the line. The velocity profile shows a nearly symmetric profile about the jet axis.

For the non-Newtonian fluid the polymer solution of 2g/L has been used, as mentioned earlier. The jet impact on the bed is consistently different from water. The viscous effect of the fluid notably influence the velocity vector patterns. Given the existence of the vortex structure in the flow, the PIV images can show its direction and magnitude. Further experiments are necessary to measure and highlight this as well as the porous effect of the particles bed. The following results show different velocity vector patterns, as shown in Fig. 11, compared from water flow. PIVLab processed 300 imported images extracted from the Samsung camera. The procedure used was the same as in water. It can be seen that the particles were easily suspended in the fluid, and obviously the time for particles to settle in non-Newtonian liquid is longer compared to in water. As the glass cell is symmetric about the jet axis a profile plot of the velocity profile is extracted about the jet axis, as seen in Fig. 12. The figure also



Figure 11: Superposition of cropped picture of the velocity vectors averaged from 300 images.

shows a profile plot of the vertical component of the velocity profile taken from jet axis to the left side of the glass cell. The line is taken 58mm above the particle bed. Figure 12 also gives evidence that the impingement of the jet on the bed creates erosion of the bed and transport particles outward. But because of the confinement of the glass cell particles are entrained by the vortex flow and spun out due to the action of centrifugal forces. The crater profile looks also different from water flow.

As seen in Fig. 13 the crater is smaller in diameter compared to with water flow. It was also observed that the depth is shallower. This is likely due to the effect of liquid rheology. Particle sticking together by PAC is enhanced and the experimental setup makes recirculation of fluid limited because of the closed system. The box is not large enough so that the jet pattern is influenced by the wall boundary conditions.

As the jet impacted the particle bed, they were swept away at the center, as mentioned earlier. The crater formation starts here and the images from the bottom becomes brighter. The crater lip, as illustrated in Fig. 2 continues to grow while the exposed area region widened. The crater is axisymmetric about the jet axis. This sit-

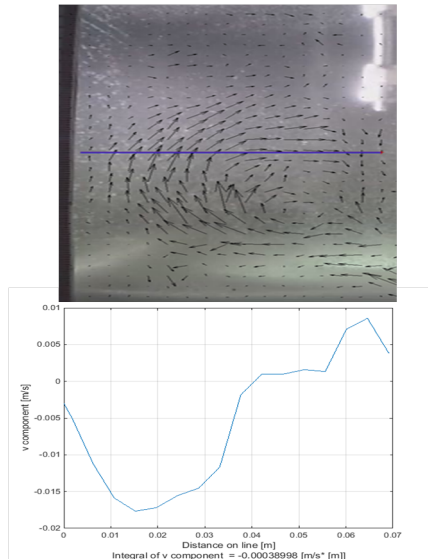


Figure 12: Top: Reference picture showing a line situated 5.8cm above the bed. Bottom: Profile plot of the vertical component of the flow.

uation is consistent with Sutherland and Dalziel².

Further experiments with other particles were not performed. Nor experiments with possibilities to measure the depth development of the crater. Therefore, analysis of the crater was difficult.

CONCLUSIONS

Experimental studies of particle suspension by jet impingement on a cohesion-

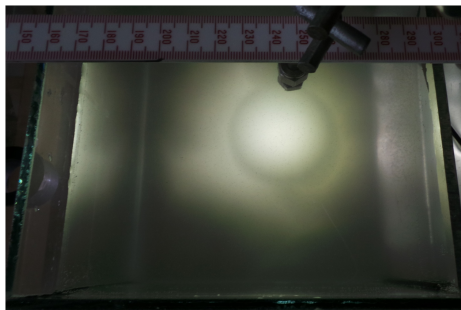


Figure 13: Top view of the scour pattern in the particle bed in non-Newtonian flow. LED light is set from below.

less particles bed are presented in this paper. 2 and 4g/L of PAC dissolved in water have been used for demonstrating the effect of non-Newtonian fluid. The results show an axisymmetric scouring of particles. PAC solution held the particles in suspension over long time compared to water flow. The analysis of PIV images revealed the flow field produced by vortex above the bed of particles.

ACKNOWLEDGEMENTS

The work was carried out at the Two Phase Flow Laboratory at the University of Stavanger, Norway. Thanks are given to Nikita Potokin for running the rheological measurements.

REFERENCES

1. Zuckerman, N. and Lior, N., (2006), Advances in Heat Transfer, 39, ISSN 0065-2717.
2. Bruce R. Sutherland and Stuart Dalziel, (2014) Physics of Fluids, 26, 035103.
3. H. Rabia, (1992), Oil Well Drilling Engineering, Graham and Trotman Ltd, ISBN 0-86010-661-6.
4. Beltaos, S. and Rajaratnam, N., (1974), "Impinging Circular Turbulent Jets." Journal Hydraulic Division, ASCE 100, pp. 1313-1328.
5. A.H. Rabenjafimanantsoa and Time Rune (2005), "Flow Regimes Over Particle beds - Experimental Studies of Particle Transport in Horizontal Pipes", Annual Transactions of the Nordic Rheology Society, Vol. 13, pp. 99-106.
6. Haehne, R.B. Cushman-Roisin and W.B. Dade (2006), "Crater Evolution due to a Jet Impinging on a Bed of Loose Particles," 11th ASCE Earth and Space Conference, March 3-6, Long Beach, CA.
7. Avidemux software. avidemux.org
8. W. Thielicke and E. J. Stamhuis (2010), "PIVlab - Time-Resolved Digital Particle Image Velocimetry Tool for MATLAB". <http://pivlab.blogspot.no/>.